Pergamon

Int. J. Solids Structures Vol. 33, No. 13, pp. 1903–1919, 1996

0020-7683/96 $15.00 + .00

0020-7683(95)00136-O

HOMOGENEOUS NUCLEATION OF A SOLID–SOLID DILATATIONAL PHASE TRANSFORMATION

B. MORAN
Department of Civil Engineering, Northwestern University, Evanston, IL 60208, U.S.A.

Y. A. CHU
Department of Mechanical Engineering, Northwestern University, Evanston, IL 60208, U.S.A.

and

G. B. OLSON
Department of Materials Science and Engineering, Northwestern University, Evanston, IL 60208, U.S.A.

(*Received* 24 *August* 1994; *in revised form* 15 *April* 1995)

Abstract—The problem of homogeneous coherent nucleation of a spherical particle in an infinite matrix is considered. A Landau–Ginzburg type potential is used to describe the material response. The underlying Landau potential is taken to be of the 2-3-4 type and the gradient energy contribution is taken to be quadratic. The nucleation problem is posed as an energy extremum problem and the finite element method, in conjunction with a perturbed Lagrangian algorithm, is used to obtain solutions with nucleus structure. The present nonlinear model spans the range from classical to nonclassical nucleation and exhibits many of the physical phenomena associated with nonclassical nucleation including divergence in radius and interface thickness of the critical nucleus and vanishing of the nucleation energy as the instability temperature is approached.

1. INTRODUCTION

An area of current interest in materials science and solid-state physics is the understanding and modeling of solid–solid phase transformations. Solid–solid phase transformations can be classified as diffusional or diffusionless. According to Cohen *et al.* (1979), diffusionless, displacive phase transformations can be further classified into shuffle transformations involving displacement of atoms, but no net strain, and lattice-distortive transformations, where one Bravais lattice is converted into another. Lattice-distortive transformations may be dilatational or deviatoric dominant. Strain energy dominated, deviatoric, lattice-distortive transformations are termed martensitic.

Several different approaches to modeling the mechanics of structural transformations have recently been pursued. Ball and James (1987) considered microstructural arrangements of martensite variants through minimizing sequences of non-convex (multiple-well) free-energy functionals. Abeyaratne and Knowles (1990) provided a theoretical basis for the description of phase boundary motion based on the concept of interface driving traction (or energetic driving force). A phase field model for phase transitions in solids has been recently developed by Fried and Gurtin (1994). An alternative approach to modeling solid state phase transitions has been in place for some time (Roitburd, 1978). The method is based on nonlinear, nonlocal elasticity and can be regarded as a Landau–Ginzburg type approach wherein the Landau potential (non-convex free-energy functional) is augmented by a gradient energy contribution resulting from a continuum description of material behavior at atomistic scales. This approach has been used to investigate behavior of shape memory alloys by Falk (1983) and to describe modulated microstructures by Barsch and Krumhansl (1984; 1988). This Landau–Ginzburg approach has also been applied to the problem of nucleation (in one-dimension) by Olson and Cohen (1982) and later elaborated upon by Haezebrouck (1987).

One of the primary issues in understanding the kinetics of structural transformations in crystalline solids is the need for quantitative information on interfacial energy and

energetics of nucleation. It is important, therefore, to develop solution techniques and solve prototype problems to address these issues. Nucleation in solids has been extensively studied within the framework of the so-called classical theory (well-defined constant strain nucleus with a sharp interface with constant surface energy). The classical nucleation model (Fisher *et al.*, 1949; Kaufman and Cohen, 1958; Christian, 1975; Porter and Easterling, 1992) is known to accurately represent nucleation behavior in the vicinity of the equilibrium temperature.† Outside this regime, and especially as the instability temperature‡ is approached, nonclassical nucleation occurs (Olson and Roitburd, 1992). Characteristic features of nonclassical nucleation in solid-state phase transformations, not predicted by classical theory, include a non-constant strain field within the nucleus, diffuse interface and divergence of the size of the critical nucleus as the instability temperature is approached.

Using the special case of homogeneous nucleation (without the aid of catalyzing defects) to address the transition between classical and nonclassical mechanisms, Landau–Ginzburg theories have been applied to model one-dimensional nucleation problems by Olson and Cohen (1982) and Haezebrouck (1987). Key features of the one-dimensional model are the specification of strain at the center of the nucleus and the availability of analytical solutions. Hong (1994) considered the spherical nucleation problem of a dilatational phase transformation but with a simpler representation of the constitutive relation—the so-called two-parabola model. Although the two-parabola model lends itself to analytical treatment, it does not reproduce critical phenomena associated with nonclassical nucleation which are observed in the one-dimensional model. Lusk (1994) discussed surface effects in dilatational phase transformations with sharp coherent interfaces. Budiansky and Truskinovsky (1993) used a simple Landau model to explore the interaction between an applied shear stress and a hydrostatic stress in tetragonal to monoclinic phase transformations.

In this paper, the problem of homogeneous coherent§ nucleation of a spherical particle in an infinite isotropic material is considered. We focus on a simple nucleation model (thermally induced dilatation) which exhibits the key features associated with both classical and nonclassical nucleation. One constitutive model, based on a Landau–Ginzburg free-energy potential, is used for the entire system, i.e., for the parent and product phases. Constitutive models of this kind are closely analogous to Cahn–Hilliard models of diffusional phase transformations. The nucleation energy is derived from the full three-dimensional nonlocal elasticity theory through appropriate symmetry considerations. Additional identities which hold for spherical symmetry and for an infinite domain are invoked to obtain an expression for the nucleation energy which depends on the dilatational strain and strain gradient only. Under appropriate restrictions on the temperature dependence of the elastic moduli, this expression is mathematically equivalent to the form of the nucleation energy obtained by Cahn and Hilliard (1959) in their treatment of nucleation in a two-component fluid. Thus the spherically symmetric displacive and diffusional nucleation problems have the same mathematical structure.

Asymptotic solutions are presented for nucleation behavior in the vicinity of the equilibrium and instability temperatures. Numerical results are presented for the full temperature range and the energy, size and structure of the critical nucleus at various temperatures are determined. The role of shear resistance or accommodation in the parent phase is investigated. The numerical results are shown to be consistent with theoretical predictions of behavior at the equilibrium and instability temperature limits.

In the following section, the spherically symmetric nucleation model is introduced and theoretical predictions of behavior at the equilibrium and instability temperatures are derived. The finite element implementation of the model is outlined in Section 3. Sample results are presented in Section 4 and a discussion and concluding remarks are given in Section 5.

† At the equilibrium temperature the potential wells associated with the parent and product phases have the same level of free-energy density.

‡ At the instability temperature the curvature of the free-energy density of the parent phase vanishes.

§ In a coherent transformation, continuity of displacements and tractions across an interface are maintained. Consequently, the accommodation of a coherent transformation is resisted by surrounding material and, in general, the resulting deformation is inhomogeneous.

2. NUCLEATION MODEL

2.1. *Nucleation energy*

The problem considered is that of coherent nucleation of a spherical particle in an infinite isotropic elastic matrix. The transformation itself is taken to be a thermally-induced dilatation and thus preserves the spherical symmetry of the problem. As will be seen below, the dilatational transformation is relatively simple to model yet it exhibits many of the features found in transformations with less symmetry. In particular, the role of shear accommodation in the parent phase is investigated. The issue of shear accommodation arises due to the inhomogeneous deformations associated with solutions with nucleus structure. The nucleation event is driven by a temperature dependent driving force associated with the difference in free-energy densities of the parent and product phases. The material is assumed to be governed by a Landau–Ginzburg free-energy which depends on strain and strain gradients. The dependence on strain gradients is a consequence of extending a continuum description to atomistic dimensions and gives rise to a characteristic length scale in the problem. The potential is assumed to be of the 2-3-4 type in dilatational strain but quadratic in the deviatoric strain and in the strain gradients. A small strain theory is employed although the methodology presented can be readily extended to account for geometric nonlinearity (see Barsch and Krumhansl, 1988, for a discussion of this theory together with application to 4 mm/2 mm ferroelastic martensite transformation and the development of modulated microstructures). The free-energy functional for an isotropic material undergoing spherically symmetric deformation at (absolute) temperature T can be written as

$$W = 4\pi \int_0^\infty [\tilde{g}(\varepsilon_{kk}, T) + \tilde{\mu} e_{ij} e_{ij} + \frac{D_1}{2}(u_{i,jk} u_{i,jk}) + \frac{D_2}{2}(u_{i,ij} u_{k,kj})] r^2 \, dr \tag{1}$$

where u_i, $\varepsilon_{ij} = (u_{i,j} + u_{j,i})/2$ and $e_{ij} = \varepsilon_{ij} - \varepsilon_{kk}\delta_{ij}/3$ are the rectangular Cartesian components of displacement, strain and deviatoric strain, respectively, and we take

$$\tilde{g}(\varepsilon_{kk}, T) = \tilde{A}(\varepsilon_{kk})^2 - \tilde{B}(\varepsilon_{kk})^3 + \tilde{C}(\varepsilon_{kk})^4. \tag{2}$$

Because the transformation is taken to be dilatational, we use a 2-3-4 type potential for the dilatational strain energy but deviatoric strain energy is taken to be quadratic. The last two terms in (1) represent the strain-gradient energy which is deduced from the strain-gradient energy for an isotropic material (Mindlin, 1965) by considering spherical symmetry (i.e., $\mathbf{u} = u(r)e_r$, for which $u_{i,jk} = u_{j,ki} = u_{k,ij}$). Note that for spherical symmetry, and if $u^2 r \to 0$ as $r \to \infty$, then the following identities‖ hold:

$$\int_0^\infty [e_{ij} e_{ij}] r^2 \, dr = \frac{2}{3} \int_0^\infty [(\varepsilon_{kk})^2] r^2 \, dr \tag{3}$$

$$\int_0^\infty [u_{i,jk} u_{i,jk}] r^2 \, dr = \int_0^\infty [u_{i,ik} u_{j,jk}] r^2 \, dr. \tag{4}$$

Now assume that $\varepsilon_{kk} = 0$ in the parent phase and define the normalized dilatation strain as $\eta = \varepsilon_{kk}/\bar{\varepsilon}_{kk}$, where $\bar{\varepsilon}_{kk}$ is the transformation strain under homogeneous deformation (i.e., η is a constant). Hence, $\eta = 0$ and $\eta = 1$ correspond to the parent and product phases of the transformation under homogeneous deformation respectively and η plays the role of an order parameter. Thus, using (3) and (4), (1) can be written as

‖ The condition for (2.4) to hold is $(u' - u/r)^2 r \to 0$ as $r \to \infty$ which is also implied by $u^2 r \to 0$ as $r \to \infty$.

$$W = 4\pi \int_0^\infty [\hat{g}(\eta, T) + \frac{\kappa}{2}(\eta')^2] r^2 \, dr \tag{5}$$

where a prime denotes differentiation with respect to r and the gradient coefficient, $\kappa = (D_1 + D_2)(\bar{\varepsilon}_{kk})^2$, is a positive quantity. Here we have introduced the quantities $\hat{g} = g + (2\mu/3)\eta^2$ and $g(\eta, T) = A\eta^2 - B\eta^3 + C\eta^4$ where $\mu = \tilde{\mu}(\bar{\varepsilon}_{kk})^2$ is the scaled shear modulus, $A = \tilde{A}(\bar{\varepsilon}_{kk})^2$, $B = \tilde{B}(\bar{\varepsilon}_{kk})^3$ and $C = \tilde{C}(\bar{\varepsilon}_{kk})^4$. The constants A, B and C are (scaled) second, third and fourth order elastic constants respectively. The form (5) is particularly advantageous from a finite element point of view in that the normalized dilatation strain η can be taken as the primary variable and standard linear finite elements can be employed as described below. If the displacement field is required, it can be simply obtained from the integral $u(r) = \bar{\varepsilon}_{kk}[\int_0^r (\eta s^2 \, ds)]/r^2$.

The driving force for a temperature-induced phase transformation is the difference in free-energy densities of the parent and product phases, which is temperature dependent. Here, we wish to maintain an analogy with the Olson–Cohen model (Olson and Cohen, 1982; Olson and Roitburd, 1992) for martensitic systems to introduce the temperature dependence of the 2-3-4 potential $g(\eta, T)$ and provide a basis for subsequent modeling of martensitic nucleation. To describe $g(\eta, T)$, we consider a special case of the transformation under homogeneous deformation (i.e., ε_{kk} constant and $e_{ij} = 0$). As mentioned above, $\eta = 0$ and $\eta = 1$ correspond to the parent and product phases under homogeneous deformation, respectively. Thus, for example, the driving force for transformation under homogeneous deformation is given by $\Delta g(T) = g(1, T) - g(0, T) = g(1, T)$, since $g(0, T) = 0$. At the equilibrium temperature, T_e, the potential wells associated with the parent and product phases have the same level of free-energy density, i.e., $g(0, T_e) = g(1, T_e)$, hence $\Delta g(T_e) = 0$. Let Δg_i denote the critical driving force at the instability temperature, T_i, i.e., $\Delta g_i = g(1, T_i) - g(0, T_i) = g(1, T_i)$. Note, at T_i, the bulk modulus of the parent phase vanishes (i.e., $(\partial^2 g/\partial \eta^2)|_{\eta=0, T=T_i} = 2A|_{T=T_i} = 0$). Now define a normalized driving force $\alpha = \Delta g(T)/\Delta g_i$. Constraining $g(\eta, T)$ to have minima at $\eta = 0$ (parent phase) and $\eta = 1$ (product phase), assuming the modulus A is linearly proportional to $(1 - \alpha)$ and defining the energy density barrier, ϕ_0, at the equilibrium temperature, T_e, the moduli A, B and C can be represented as

$$\begin{aligned} A/\phi_0 &= 16(1-\alpha) \\ B/\phi_0 &= 32(1-\alpha) - 4\alpha\beta \\ C/\phi_0 &= 16(1-\alpha) - 3\alpha\beta \end{aligned} \tag{6}$$

where $\beta = \Delta g_i/\phi_0$. The dependence of the 2-3-4 potential function $g(\eta)$ on the normalized driving force α is depicted in Fig. 1. The effect of increasing α is to reduce the energy density barrier ϕ and to soften the moduli A, B and C. The temperature dependencies of moduli A, B and C are introduced through the temperature dependence of the normalized driving force α (e.g., $\alpha = (T - T_e)/(T_i - T_e)$). The first terms on the right hand sides of (6) imply the temperature (or α) dependence of the bulk modulus, $2A$, of the parent phase and the second terms (for moduli B and C) the temperature (or α) dependence of the driving force. Here, we have linear α dependence for both quantities for simplicity.

For transformations under inhomogeneous deformation (i.e., those with nucleus structure), the deviatoric strain energy is non-zero and the energy functional (5) is used. In this case, the 2-3-4 potential $\hat{g}(\eta, T)$ has minima at $\eta = 0$ (parent phase) and $\eta = \eta_m$ (product phase) where

$$\eta_m = \frac{3B + \sqrt{9B^2 - 32\hat{A}C}}{8C} \tag{7}$$

where $\hat{A} = A + 2\mu/3$. Since the modulus A is equal to one half the bulk modulus of the parent phase, the Poisson's ratio of the parent phase, ν, can be represented as

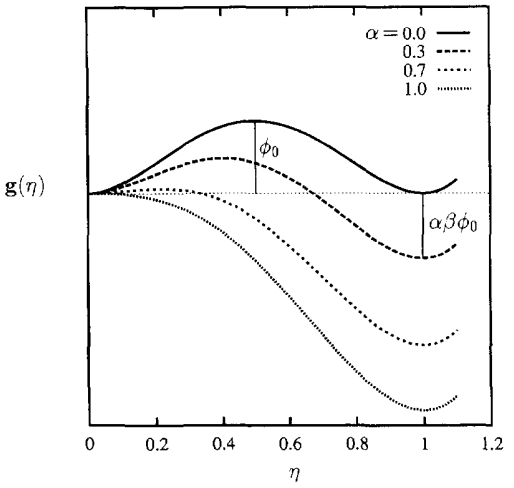

Fig. 1. Landau 2-3-4 potential $g(\eta)$ for different values of normalized driving force α.

$\nu = (3-\mu/A)/(6+\mu/A)$, which is temperature (or α) dependent if the moduli A and μ have different temperature (or α) dependencies. The initial Poisson's ratio, ν_0, is defined as the Poisson's ratio of the parent phase evaluated at $\alpha = 0$.

The value of α corresponding to a transformation under inhomogeneous deformation at the instability temperature is obtained from the condition $\hat{A} = 0$ and is denoted as α_i. The value of α_i depends on the initial Poisson's ratio and the temperature dependencies of the moduli A and μ. Due to the shear resistance, the dilatational transformation under inhomogeneous deformation first occurs at a value of $\alpha = \alpha_c$ corresponding to the coherent equilibrium temperature,¶ T_c. Since $\hat{g}(0, T_c) = 0$, the value of α_c is obtained from the condition $\hat{g}(\eta_m, T_c) = 0$ and depends not only on the initial Poisson's ratio and the temperature dependencies of the moduli A and μ but also on the value of β.

It is noted that the form of (5) is analogous to that considered by Cahn and Hilliard (1959) in their treatment of nucleation in a two-component fluid. It will be shown later that the nucleation model proposed here predicts the same asymptotic solutions as Cahn–Hilliard's at the coherent equilibrium and instability temperatures.

2.2. *Nucleation problem*

The nucleation problem is posed as an energy extremum problem. The energy associated with the formation of a nucleus, with strain profile $\eta(r)$, is given by (5). It can be seen from (5) that the energy associated with constant strain profiles (without nucleus structure) for which $(\mathrm{d}\hat{g}/\mathrm{d}\eta) = 0$ and $\eta' = 0$ will be extrema but violate the assumption of $u^2 r \to 0$ as $r \to \infty$ (required for the use of (3) and (4)) except the one $\eta(r) = 0$ which is not of interest to the nucleation problem considered here. However an additional extremum of (5) exists for which a non-constant strain profile, $\eta(r)$, is obtained. This extremum yields a local energy minimum of W (Alexiades and Aifantis, 1986) with respect to $\eta(r)$ and corresponds to the critical nucleus which is in unstable equilibrium with respect to the nucleus size. The strain profile corresponding to the critical nucleus is referred to as the structure of the critical nucleus and the associated energy is called the minimum nucleation energy barrier. A finite element method, in conjunction with a perturbed Lagrangian algorithm is used to obtain the critical nucleus solution.** To motivate the solution procedure, we first consider the stationarity of the Landau–Ginzburg potential (5). After discussion of the governing equation and appropriate boundary conditions for the nucleation problem, we discuss the theoretical predictions for nucleation behavior close to the coherent equilibrium temperature ($\alpha = \alpha_c$) and the instability temperature ($\alpha = \alpha_i$). The perturbed Lagrangian

¶ At the coherent equilibrium temperature $\hat{g}(0, T_c) = \hat{g}(\eta_m, T_c)$.

** As will be seen below, the critical nucleus can be obtained through solution of a two-point boundary value problem with an integral constraint. We choose to use the finite element method to solve this problem in anticipation of future applications of this and related Galerkin methods to the martenistic nucleation problem.

method is then introduced as a means of obtaining non-trivial (critical nucleus) solutions for values of α in the range from α_c to α_i.

Taking the variation of (5) with respect to η and applying the divergence theorem gives

$$\delta W = 0 = \int_0^\infty \delta\eta \left[\frac{\mathrm{d}\hat{g}(\eta)}{\mathrm{d}\eta} - \kappa \frac{\mathrm{d}^2\eta}{\mathrm{d}r^2} - \frac{2\kappa}{r}\frac{\mathrm{d}\eta}{\mathrm{d}r} \right] r^2 \,\mathrm{d}r + \delta\eta \left(\kappa \frac{\mathrm{d}\eta}{\mathrm{d}r} r^2 \right) \Big|_0^\infty \tag{8}$$

and the associated Euler–Lagrange equation is given by

$$\kappa \frac{\mathrm{d}^2\eta}{\mathrm{d}r^2} + \frac{2\kappa}{r}\frac{\mathrm{d}\eta}{\mathrm{d}r} = \frac{\mathrm{d}\hat{g}(\eta)}{\mathrm{d}\eta}. \tag{9}$$

It can be seen from (8) that the presence of the r^2 term precludes the specification of either essential or natural boundary conditions at $r = 0$. Unlike in the one-dimensional problem (Olson and Cohen, 1982), the normalized strain η can not therefore be specified at $r = 0$ to obtain non-trivial (i.e. those with a nucleus structure) solutions to (9). We assume that the strain field is uniform at infinity and thus the boundary condition for the Euler–Lagrange eqn (9) is given by

$$\frac{\mathrm{d}\eta}{\mathrm{d}r} r^2 \Big|_{r=\infty} = 0. \tag{10}$$

For (3) and (4) to hold, the solution should also satisfy the following condition

$$u^2 r|_{r=\infty} = 0 \tag{11}$$

which also implies the parent phase at infinity (i.e., $\eta(\infty) = 0$).

As mentioned above, there is a constant (trivial) solution of the Euler–Lagrange eqn (9) subject to the boundary conditions (10) and (11), i.e., $\eta(r) = 0$, and for which $\hat{g}(\eta)$ has a minimum, but we are interested in the non-trivial solution which is in meta-stable equilibrium with respect to strain perturbation but unstable with respect to the nucleus size. Hence, the strain profile associated with this solution represents a critical nucleus. The energy associated with the critical nucleus is the minimum nucleation energy barrier, which is a local minimum of (5) with respect to $\eta(r)$ but a maximum with respect to the nucleus size. Before we introduce the perturbed Lagrangian method to obtain the critical nucleus solution, we discuss the asymptotic solutions close to the coherent equilibrium and instability temperatures to show that the model can span the range from classical to nonclassical nucleation.

2.3. *Solutions near the instability and equilibrium*

Close to the instability temperature ($\alpha \to \alpha_i$), the normalized strain profile $\eta(r) \to 0$, since the energy density barrier, $\hat{\phi}$ (the maximum of $\hat{g}$), is close to zero. Following an analogous procedure to that of Cahn and Hilliard (1959), (5) can be rewritten as

$$W_{(\alpha \to \alpha_i)} = 4\pi \int_0^\infty [\hat{A}\eta^2 - B\eta^3 + \frac{\kappa}{2}(\eta')^2] r^2 \,\mathrm{d}r \tag{12}$$

by neglecting the fourth order term in $\hat{g}(\eta)$. Introducing the parameters

$$Y = \frac{B}{\hat{A}}\eta \tag{13}$$

and

$$t = \left(\frac{2\hat{A}}{\kappa}\right)^{1/2} r \tag{14}$$

(12) can be rewritten as

$$W_{(\alpha\to\alpha_i)} = 4\pi\left(\frac{2}{\kappa}\right)^{-3/2} \hat{A}^{3/2} B^{-2} \int_0^{\infty} \left[Y^2 - Y^3 + \left(\frac{\mathrm{d}Y}{\mathrm{d}t}\right)^2 \right] t^2 \,\mathrm{d}t. \tag{15}$$

Because the integral in (15) is dimensionless and independent of α and also noting that $\hat{A} \to 0$ but B remains finite as $\alpha \to \alpha_i$, for constant κ, it can be shown that

$$W_{(\alpha\to\alpha_i)} \sim (\alpha_i - \alpha)^{3/2}. \tag{16}$$

If we define the radius, R, of the critical nucleus by $|\eta'|_{r=R} = |\eta'|_{max}$, which means that the maximum strain gradient occurs at $r = R$, then it can also be shown that

$$R_{(\alpha\to\alpha_i)} \sim (\alpha_i - \alpha)^{-1/2}. \tag{17}$$

It can be seen from (16) and (17) that, as $\alpha \to \alpha_i$, the nucleation energy tends to zero but the radius of the critical nucleus tends to infinity. This behavior is associated with the nonclassical nucleation but is not predicted by the classical nucleation theory. The exponents in (16) and (17) are consistent with the results of Cahn and Hilliard (1959) who considered nucleation in a two-component fluid.

Close to the coherent equilibrium temperature ($\alpha \to \alpha_c$), it can be assumed that the radius of the critical nucleus is large compared with the interface thickness and that the strain within the nucleus is constant, then the strain gradient in (5) can be assumed constant within the interface thickness and zero elsewhere. In this case, the present model reduces to that of the classical theory and it can be shown that

$$W_{(\alpha\to\alpha_c)} = \frac{16\pi\Gamma^3}{3\hat{g}(\eta_m)^2} \tag{18}$$

and

$$R_{(\alpha\to\alpha_c)} = -\frac{2\Gamma}{\hat{g}(\eta_m)} \tag{19}$$

where Γ is the *surface energy*. Since $\hat{g}(\eta_m)$ is a function of α and $\hat{g}(\eta_m) = 0$ at $\alpha = \alpha_c$, expanding $\hat{g}(\eta_m)$ about α_c and neglecting the higher order terms in $(\alpha - \alpha_c)$, it can be shown that $\hat{g}(\eta_m) \sim (\alpha - \alpha_c)$ as $\alpha \to \alpha_c$ and

$$W_{(\alpha\to\alpha_c)} \sim (\alpha - \alpha_c)^{-2} \tag{20}$$

and

$$R_{(\alpha\to\alpha_c)} \sim (\alpha - \alpha_c)^{-1}. \tag{21}$$

Following the definition by Olson and Cohen (1982), the interface thickness, δ, mentioned above is defined as

$$\delta = \frac{\eta(0)}{|\eta'|_{\max}}. \tag{22}$$

It can also be shown that the interface thickness, δ_c, at the coherent equilibrium temperature can be represented by

$$\delta_c = \left(\sqrt{\frac{\kappa}{2C}}\frac{8C}{B}\right)\Bigg|_{\alpha=\alpha_c} \tag{23}$$

which is used as the characteristic length scale for the nucleation problem. Introducing the parameters

$$\tilde{\eta} = \frac{\eta}{\eta_m} \tag{24}$$

and

$$\tilde{t} = \left(\frac{2C}{\kappa}\right)^{1/2} \eta_m r \tag{25}$$

substituting (24), (25) into (5) and also applying (7) and (23), the nucleation energy at the coherent equilibrium temperature can be represented as

$$W_{(\alpha=\alpha_c)} = \pi\hat{\phi}_c\delta_c^3 \int_0^\infty \left[\tilde{\eta}^2 - 2\tilde{\eta}^3 + \tilde{\eta}^4 + \left(\frac{\mathrm{d}\tilde{\eta}}{\mathrm{d}\tilde{t}}\right)^2\right]\tilde{t}^2\,\mathrm{d}\tilde{t} \tag{26}$$

where

$$\hat{\phi}_c = C\left(\frac{B}{4C}\right)^4\Bigg|_{\alpha=\alpha_c} \tag{27}$$

is the energy density barrier at $\alpha = \alpha_c$. Since the integral in (26) is dimensionless, this implies that the solution $\tilde{\eta}(\tilde{t})$ of the Euler–Lagrange equation associated with (26) is independent of the material moduli. The quantity $\hat{\phi}_c\delta_c^3$ can thus be used as the nucleation energy scale. The quantity $\tilde{\eta}$ defined in (24) plays the role of an order parameter. Hence, $\tilde{\eta} = 0$ and $\tilde{\eta} = 1$ correspond to the parent and product phases of dilatation transformation under inhomogeneous deformation, respectively. It should be noted that $\tilde{\eta}$ and η are different order parameters; the latter is an order parameter for dilatational transformation under homogeneous deformation. A quantity of interest is $\tilde{\eta}(0)$, the normalized strain in the critical nucleus at $r = 0$, which is representative of the nucleus structure. For strongly classical nucleation, $\tilde{\eta}(0) \approx 1$ while for strongly nonclassical nucleation $\tilde{\eta}(0) \approx 0$.

2.4. *Perturbed Lagrangian method*

A perturbed Lagrangian method is introduced to obtain the critical nucleus solution. First we note that any non-trivial solution satisfies the following condition for some $\bar{\eta}$ and $\bar{R}$

$$\int_0^\infty (\eta - \bar{\eta})H(\bar{R} - r)r^2\,\mathrm{d}r = 0 \tag{28}$$

where $\bar{\eta}$ is the volume average of the normalized dilatation strain η within a sphere of radius

$\bar{R}$ and H is the Heaviside step function. The perturbed Lagrangian consists of the nucleation energy (5) together with the constraint (28) and is written as

$$\mathscr{W} = 4\pi\left\{\int_0^\infty \left[\hat{g}(\eta) + \frac{\kappa}{2}(\eta')^2\right] r^2\,\mathrm{d}r + \int_0^\infty \lambda(\eta-\bar{\eta})H(\bar{R}-r)r^2\,\mathrm{d}r - \frac{1}{2\gamma}\lambda^2\right\} \tag{29}$$

where λ is a Lagrange multiplier and γ is a large positive constant. Taking the variation of (29) with respect to η and λ yields two Euler–Lagrange equations

$$\kappa\frac{\mathrm{d}^2\eta}{\mathrm{d}r^2} + \frac{2\kappa}{r}\frac{\mathrm{d}\eta}{\mathrm{d}r} = \frac{\mathrm{d}\hat{g}(\eta)}{\mathrm{d}\eta} + \lambda H(\bar{R}-r) \tag{30}$$

and

$$\int_0^\infty (\eta-\bar{\eta})H(\bar{R}-r)r^2\,\mathrm{d}r = \frac{\lambda}{\gamma}. \tag{31}$$

The boundary condition is the same as (10) and the non-trivial solution we seek is that which in addition satisfies (11). Since γ is a large constant, (31) is equivalent to (28) as long as the value of λ is small compared to γ (i.e., $\lambda \ll \gamma$). However, only at $\lambda = 0$, is the solution of (30) equivalent to the non-trivial solution of (9). Hence, to obtain the strain profile of the critical nucleus it is required to solve (30) and (31) subject to (10) and (11) and for values of $\bar{\eta}$ and $\bar{R}$ that make $\lambda = 0$. This procedure is carried out by means of the finite element method which is described in the following section.

3. FINITE ELEMENT IMPLEMENTATION

The variation of (29), or the weak form of (30–31), is written as

$$\delta\mathscr{W} = 0 = \int_0^\infty \left[\frac{\mathrm{d}\hat{g}(\eta)}{\mathrm{d}\eta}\delta\eta + \kappa\eta'\delta\eta' + \lambda H(\bar{R}-r)\delta\eta\right] r^2\,\mathrm{d}r + \delta\lambda\left[\int_0^\infty (\eta-\bar{\eta})H(\bar{R}-r)r^2\,\mathrm{d}r - \frac{1}{\gamma}\lambda\right]. \tag{32}$$

The finite element implementation of the weak form (32) follows standard procedures but with the normalized dilatation strain η and the Lagrange multiplier λ taken as the primary variables. Using standard isoparametric elements we write

$$\eta_e = \sum_{a=1}^{2} N_a(\xi(r))\eta_a^e = \mathbf{N}\mathbf{d}_e \tag{33}$$

for strains within an element. The strain gradients within an element are given by

$$\eta_e' = \sum_{a=1}^{2} N_{a,\xi}(\xi(r))\xi_{,r}\eta_a^e = \mathbf{B}\mathbf{d}_e. \tag{34}$$

The weak form (32) requires only a linear variation of η within an element and we choose standard two-node linear elements. Writing similar interpolation relations for the variations, substituting into the incremental form of (32), allowing for the arbitrariness of nodal and Lagrange multiplier variations and using a standard Newton–Raphson procedure yields

$$\mathbf{K}_T(\tilde{\mathbf{d}}^n)\Delta\tilde{\mathbf{d}}^n = -f(\tilde{\mathbf{d}}^n)$$

$$\tilde{\mathbf{d}}^n = \begin{Bmatrix} \mathbf{d}^n \\ \lambda^n \end{Bmatrix} = \begin{Bmatrix} \Sigma_e \mathbf{N}\mathbf{d}_e^n \\ \lambda^n \end{Bmatrix} \quad \Delta\tilde{\mathbf{d}}^n = \begin{Bmatrix} \Delta\mathbf{d}^n \\ \Delta\lambda^n \end{Bmatrix} = \begin{Bmatrix} \Sigma_e \mathbf{N}\Delta\mathbf{d}_e^n \\ \Delta\lambda^n \end{Bmatrix}$$

$$f(\tilde{\mathbf{d}}^n) = \begin{Bmatrix} \Sigma_e \int_{\Omega_e} \left[\mathbf{N}^T \left(\dfrac{\mathrm{d}\hat{g}(\eta_e)}{\mathrm{d}\eta} + \lambda H(\bar{R}-r) \right) + \mathbf{B}^T \kappa \eta_e' \right]_n r^2 \, \mathrm{d}r \\ \int_0^\infty (\eta(\mathbf{d}^n) - \bar{\eta}) H(\bar{R}-r) r^2 \, \mathrm{d}r - \dfrac{1}{\gamma}\lambda^n \end{Bmatrix}$$

$$\mathbf{K}_T(\tilde{\mathbf{d}}^n) = \left[\frac{\partial f(\tilde{\mathbf{d}})}{\partial \mathbf{d}} \quad \frac{\partial f(\tilde{\mathbf{d}})}{\partial \lambda} \right]_n$$

$$= \begin{bmatrix} \Sigma_e \int_{\Omega_e} \left[\dfrac{\mathrm{d}^2 \hat{g}(\eta_e)}{\mathrm{d}\eta^2} \mathbf{N}^T\mathbf{N} + \kappa \mathbf{B}^T\mathbf{B} \right]_n r^2 \, \mathrm{d}r & \Sigma_e \int_{\Omega_e} \mathbf{N}^T H(\bar{R}-r) r^2 \, \mathrm{d}r \\ \Sigma_e \int_{\Omega_e} \mathbf{N} H(\bar{R}-r) r^2 \, \mathrm{d}r & -\dfrac{1}{\gamma} \end{bmatrix} \tag{35}$$

which is solved for the increment in nodal dilatational strains, $\Delta\mathbf{d}^n$, and in Lagrange multiplier, $\Delta\lambda^n$, at the n^{th} iteration. The nodal quantities, $\mathbf{d}$, and Lagrange multiplier, λ, are updated as $\tilde{\mathbf{d}}^{n+1} = \tilde{\mathbf{d}}^n + \Delta\tilde{\mathbf{d}}^n$ and iteration proceeds until the residual vanishes to within a desired tolerance. Recall that the non-trivial solution corresponding to the critical nucleus is that for which $\lambda = 0$. A simple procedure to search for the non-trivial solution is conducted by picking an appropriate value of $\bar{\eta}$ and varying $\bar{R}$ to solve (35) until a solution for which $\lambda = 0$ to within a sufficient tolerance is obtained. The appropriate value of $\bar{\eta}$ should be large enough in order to obtain the desired solution. In our analyses, we choose $\bar{\eta}$ to be close to η^* where η^* is such that $\hat{g}(\eta^*) = 0$, $\hat{g}'(\eta^*) < 0$. The value of η^* depends on the normalized driving force α. In the following section, results are presented for the critical nuclei as a function of driving force α for different values of initial Poisson's ratio.

4. RESULTS

Calculations were carried out for different values of normalized driving force, α, within the range of α from α_c to α_i. The relevant material parameter is $\beta = -3.0$. Two temperature dependencies for the shear modulus are considered through the normalized driving force α. One assumes the same linear α dependence as the modulus A, i.e. $\mu = \mu_0(1-\alpha)$, another assumes constant shear modulus, i.e. $\mu = \mu_0$, where μ_0 is the initial shear modulus at $\alpha = 0$. Different values of the initial Poisson's ratio $\nu_0 = 0.3$, 0.4, 0.45 and 0.5 were chosen to demonstrate the influence of the deviatoric deformation on the nucleation behavior of the dilatational transformation.

In Fig. 2, the normalized strain profiles $\tilde{\eta}(r)$, defined in (24), for critical nuclei are plotted as a function of r/δ_c for different values of normalized driving force, α, with linearly α dependent shear modulus and initial Poisson's ratio $\nu_0 = 0.3$. The associated values of the normalized driving force at the coherent equilibrium and instability temperatures are $\alpha_c = 0.7318$ and $\alpha_i = 1$, respectively.

It can be seen from the figure that, as $\alpha \to \alpha_c$, for example $\alpha = 0.75$, the normalized strain is uniform within the nucleus with a sharp decrease in strain over a narrow range—indicating a somewhat sharp interface. In contrast, as $\alpha \to \alpha_i$ (for example $\alpha = 0.99$), the normalized strain profile is non-uniform within the nucleus and the strain transition occurs over a broader range—indicating a more diffuse interface. The intermediate cases, $\alpha = 0.85$ and $\alpha = 0.95$, have non-uniform strain profiles and relatively sharp interface thicknesses. The case $\alpha = 0.75$ is representative of strongly classical nucleation which has a fully developed product phase nucleus ($\eta = \eta_m$) and a sharp interface. The case $\alpha = 0.99$ is

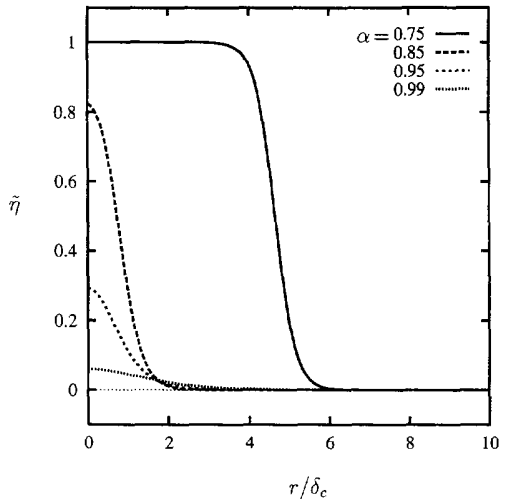

Fig. 2. Normalized strain profiles for critical nuclei, $\tilde{\eta}(r)$, for different values of normalized driving force α with linearly α dependent shear modulus and $\nu_0 = 0.3$.

representative of strongly nonclassical nucleation which has a nucleus structure close to that of the parent phase and a diffuse interface.

In Fig. 3(a), the normalized center strain $\tilde{\eta}(0)$ for the critical nucleus is plotted as a function of normalized driving force, α, with linearly α dependent shear modulus and the values of initial Poisson's ratio $\nu_0 = 0.3$, 0.4 and 0.5 which have corresponding values of $\alpha_c = 0.7318$, 0.5711 and 0 respectively and the same value of $\alpha_i = 1$. The reason that α_c depends on Poisson's ratio is that deviatoric deformation of the matrix (associated with the inhomogeneous dilatational strain field of the critical nucleus) costs energy. Since the ratio of the shear modulus to the bulk modulus decreases as the Poisson's ratio increases, the required driving force decreases as the Poisson's ratio increases. Each curve in Fig. 3(a) starts from its associated value of $\alpha = \alpha_c$ and ends at $\alpha = 1$, since there is no nucleation for $\alpha < \alpha_c$ and both the bulk and shear moduli vanish at $\alpha = 1$. The normalized center strain decreases as driving force increases. As $\alpha \to \alpha_c$, the spherical nucleus structure, which has $\tilde{\eta}(0) = 1$, can be considered as strongly classical, i.e. the nucleus center strain is identical to that of the fully developed product structure. It should be noted that the value of η_m depends on Poisson's ratio and α. As $\alpha \to 1$, the nucleus structure, which has $\tilde{\eta}(0) \to 0$, becomes indistinguishable from the parent structure and the behavior is strongly nonclassical. Following the classification of nucleation based on the normalized center strain by Olson and Roitburd (1992), a dashed line with $\tilde{\eta}(0) = 0.5$ is plotted for reference and classification in Fig. 3(a). For $\tilde{\eta}(0) > 0.5$, the nucleus structure is closer to the product phase than to the parent phase and the behavior can be regarded as a modification of classical nucleation. For $\tilde{\eta}(0) < 0.5$, the nucleus structure is closer to the parent phase than to the product phase and the behavior is strongly nonclassical. It can be seen from Fig. 3(a) that the material with a lower value of Poisson's ratio requires a higher driving force for nonclassical nucleation, which means that the nucleation of a dilatational transformation becomes more classical as the ratio of the shear modulus to the bulk modulus increases. Hence, the case $\nu_0 = 0.5$, for which $\mu/A = 0$, is the most nonclassical.

In Fig. 3(b), the normalized center strain $\tilde{\eta}(0)$ for the critical nucleus is plotted as a function of normalized driving force, α, with the initial Poisson's ratio $\nu_0 = 0.45$ for different temperature dependencies in the shear modulus. The values of α_c are 0.4025 and 0.632 for linearly α dependent and constant shear moduli, respectively. The values of α_i are 1.0 and 1.14 for linearly α dependent and constant shear moduli respectively. Note that the bulk modulus vanishes at $\alpha = 1$ and becomes negative for $\alpha > 1$. Mathematically, based on the model proposed here, $\tilde{\eta}(0) \to 0$ as $\alpha \to \alpha_i$ for the case of constant shear modulus. For $\nu_0 = 0.45$, and for the constant shear modulus case, classical nucleation (i.e., $\tilde{\eta}(0) > 0.5$)

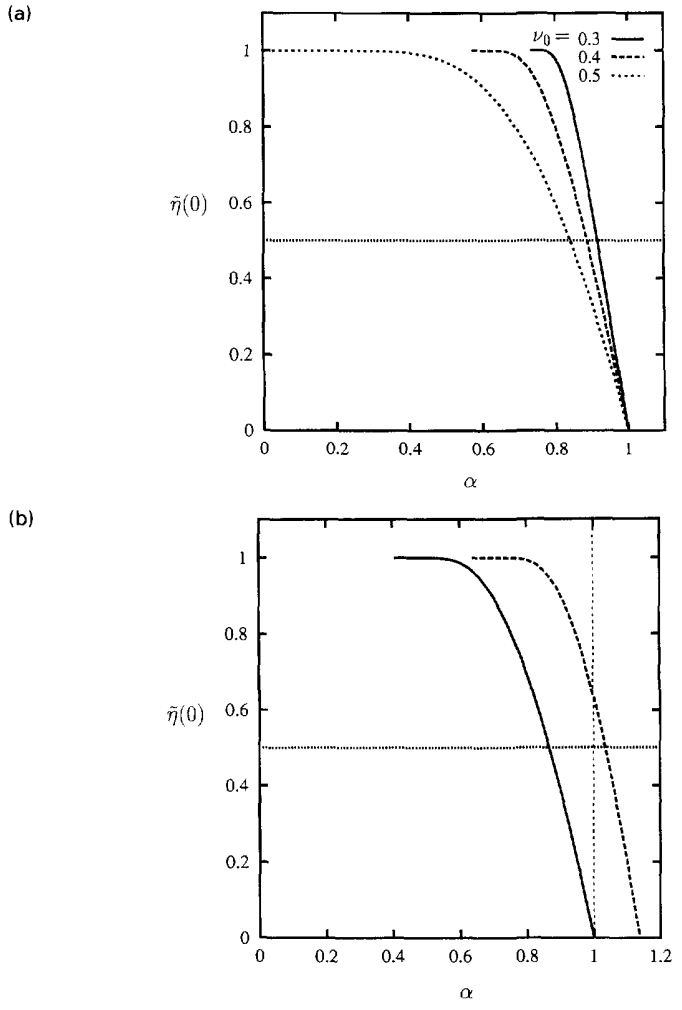

Fig. 3. (a) Normalized center strain $\tilde{\eta}(0)$ for the critical nucleus as a function of normalized driving force α with linearly α dependent shear modulus for $\nu_0 = 0.3$, 0.4 and 0.5. (b) Normalized center strain $\tilde{\eta}(0)$ for the critical nucleus as a function of normalized driving force α with $\nu_0 = 0.45$; the solid line for $\mu = \mu_0(1-\alpha)$ and the dashed line for $\mu = \mu_0$.

only is observed for the range $0 \leqslant \alpha \leqslant 1$. For higher values of initial Poisson's ratio, nonclassical nucleation (i.e., $\tilde{\eta}(0) < 0.5$) would be observed in the range $0 \leqslant \alpha \leqslant 1$.

In Fig. 4(a), the radius R of the critical nucleus, normalized with respect to the length scale δ_c, defined in (23), is plotted as a function of normalized driving force, α, with linearly α dependent shear modulus and for the values of initial Poisson's ratio $\nu_0 = 0.3$, 0.4 and 0.5. The radius of the critical nucleus, which is infinite at the coherent equilibrium temperature ($\alpha = \alpha_c$), is seen to decrease initially to a minimum, then to increase and become infinite again at the instability temperature ($\alpha = \alpha_i$) for all three cases. The phenomena close to the coherent equilibrium and instability temperatures are consistent with the theoretical predictions. Close to the coherent equilibrium temperature, the critical radius depends on the normalized driving force according to $R \sim (\alpha - \alpha_c)^{-1.0}$. The exponent is based on our numerical results of $R/\delta_c = 37.57$ and 25.75 at $\alpha = 0.734$ and 0.735, respectively, for $\nu_0 = 0.3$; $R/\delta_c = 45.24$ and 19.67 at $\alpha = 0.575$ and 0.58, respectively, for $\nu_0 = 0.4$ and $R/\delta_c = 88.71$ and 44.25 at $\alpha = 0.01$ and 0.02, respectively, for $\nu_0 = 0.5$. The value of the exponent is equal to our theoretical prediction, -1, which is consistent with the classical nucleation theory. Close to the instability temperature, we have $R \sim (1-\alpha)^m$ where $m = -0.49$, -0.50 and -0.49 for $\nu_0 = 0.3$, 0.4 and 0.5 respectively, based on the numerical data of $R/\delta_c = 2.605$ and 3.657 for $\nu_0 = 0.3$, $R/\delta_c = 3.279$ and 4.631 for $\nu_0 = 0.4$ and $R/\delta_c = 5.017$ and 7.067 for $\nu_0 = 0.5$ at $\alpha = 0.998$ and 0.999 respectively. The values of the

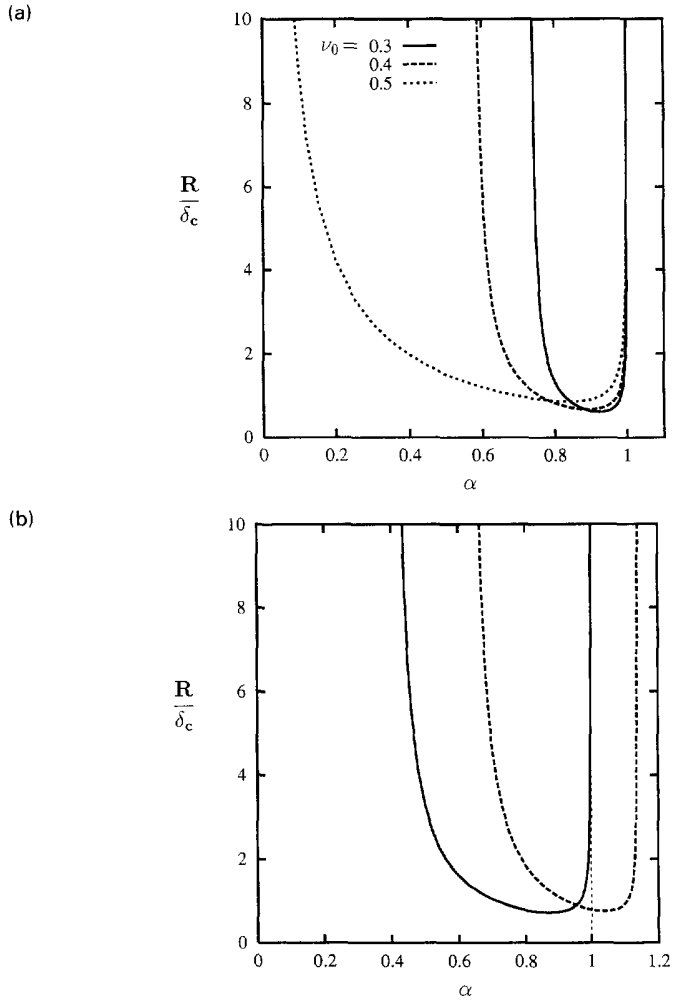

Fig. 4. (a) Radius R of the critical nucleus, normalized with respect to δ_c, as a function of normalized driving force α with linearly α dependent shear modulus for $\nu_0 = 0.3$, 0.4 and 0.5. (b) Radius R of the critical nucleus, normalized with respect to δ_c, as a function of normalized driving force α with $\nu_0 = 0.45$; the solid line for $\mu = \mu_0(1-\alpha)$ and the dashed line for $\mu = \mu_0$.

exponents are very close to our theoretical prediction, -0.5, which is consistent with the well-known nonlocal Cahn–Hilliard theory (Cahn and Hilliard, 1959). The phenomenon of $R \to \infty$ as $\alpha \to 1$, observed here, is an expected feature of the nonclassical nucleation. This phenomenon is not observed in the simpler two-parabola model of Hong, 1994.

In Fig. 4(b), the radius R of the critical nucleus, normalized with respect to the length scale δ_c, is plotted as a function of normalized driving force, α, with $\nu_0 = 0.45$ for different temperature dependencies in the shear modulus. The radius does not go to infinity at $\alpha = 1$ for the constant shear modulus case. As mentioned above, the bulk modulus vanishes at $\alpha = 1$, but in this case the effective modulus $\hat{A}$ does not vanish until $\alpha = \alpha_i > 1$. As shown in the figure, the radius does go to infinity as $\alpha \to \alpha_i$. Close to the coherent equilibrium temperature, the critical radius depends on the normalized driving force according to $R \sim (\alpha - \alpha_c)^{-1.0}$. The exponent is based on our numerical results of $R/\delta_c = 57.46$ and 27.35 at $\alpha = 0.408$ and 0.414 respectively for linearly α dependent shear modulus and $R/\delta_c = 40.58$ and 24.92 at $\alpha = 0.64$ and 0.645 respectively for constant shear modulus. Both cases are consistent with the theoretical prediction.

In Fig. 5(a), the effective interface thickness δ of the critical nucleus, normalized with respect to δ_c, is plotted as a function of normalized driving force, α, with linearly α dependent shear modulus and the values of initial Poisson's $\nu_0 = 0.3$, 0.4 and 0.5. The value of δ/δ_c, approaches unity as $\alpha \to \alpha_c$, increases gradually initially and then increases rapidly as the

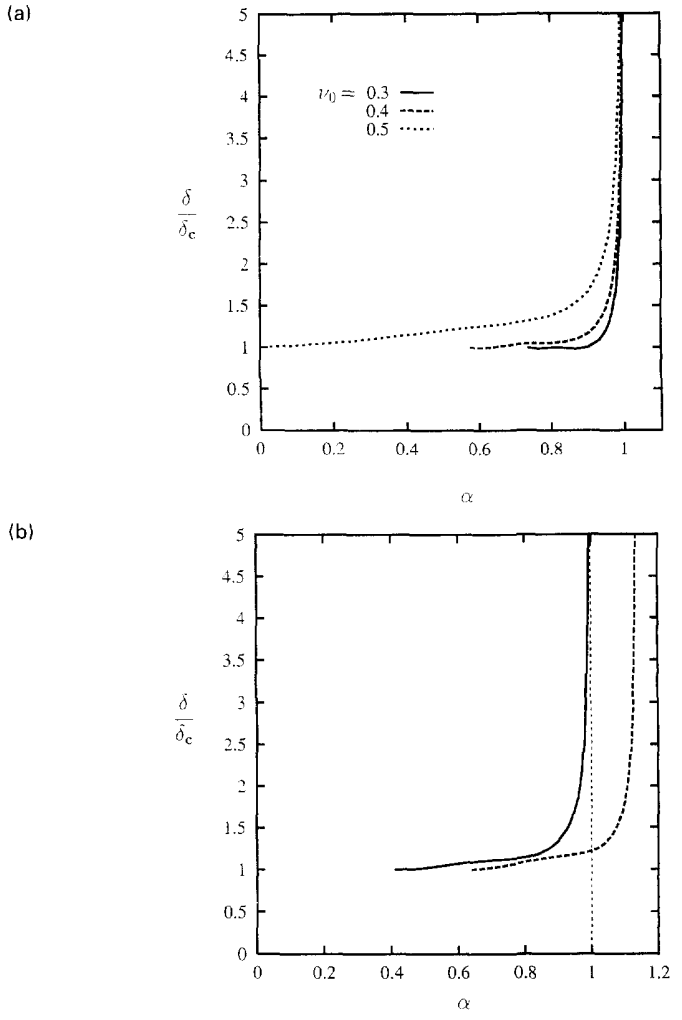

Fig. 5. (a) Effective interface thickness δ, normalized with respect to δ_c, as a function of normalized driving force α with linearly α dependent shear modulus for $\nu_0 = 0.3$, 0.4 and 0.5. (b) Effective interface thickness δ, normalized with respect to δ_c, as a function of normalized driving force α with $\nu_0 = 0.45$; the solid line for $\mu = \mu_0(1-\alpha)$ and the dashed line for $\mu = \mu_0$.

instability temperature ($\alpha = \alpha_i = 1$) is approached. The case with the higher initial Poisson's ratio has a thicker interface, which means that it behaves in a more nonclassical fashion. Close to the instability temperature, the effective interface thickness has the same rate of divergence as the critical radius i.e. $\delta \sim (1-\alpha)^m$ where $m = -0.48$, -0.50 and -0.49 for $\nu_0 = 0.3$, 0.4 and 0.5 respectively, based on the numerical data of $\delta/\delta_c = 5.30$ and 7.40 for $\nu_0 = 0.3$; $\delta/\delta_c = 6.69$ and 9.43 for $\nu_0 = 0.4$ and $\delta/\delta_c = 10.15$ and 14.27 for $\nu_0 = 0.5$ at $\alpha = 0.998$ and 0.999 respectively.

In Fig. 5(b), the effective interface thickness δ of the critical nucleus, normalized with respect to δ_c, is plotted as a function of normalized driving force, α, with the initial Poisson's ratio $\nu_0 = 0.45$ for different temperature dependencies in the shear modulus. As seen from the figure, the interface thickness does not go to infinity at $\alpha = 1$ for the case of constant shear modulus. For both cases, the values of δ/δ_c approach unity at $\alpha \to \alpha_c$.

In Fig. 6(a), the nucleation energy W of the critical nucleus, normalized with respect to $\hat{\phi}_c \delta_c^3$, is plotted as a function of normalized driving force, α, with linearly α dependent shear modulus and the values of initial Poisson's ratio $\nu_0 = 0.3$, 0.4 and 0.5. The nucleation energy barrier is infinite at the coherent equilibrium temperature ($\alpha = \alpha_c$), but decreases rapidly as the driving force increases and tends to zero as the instability temperature

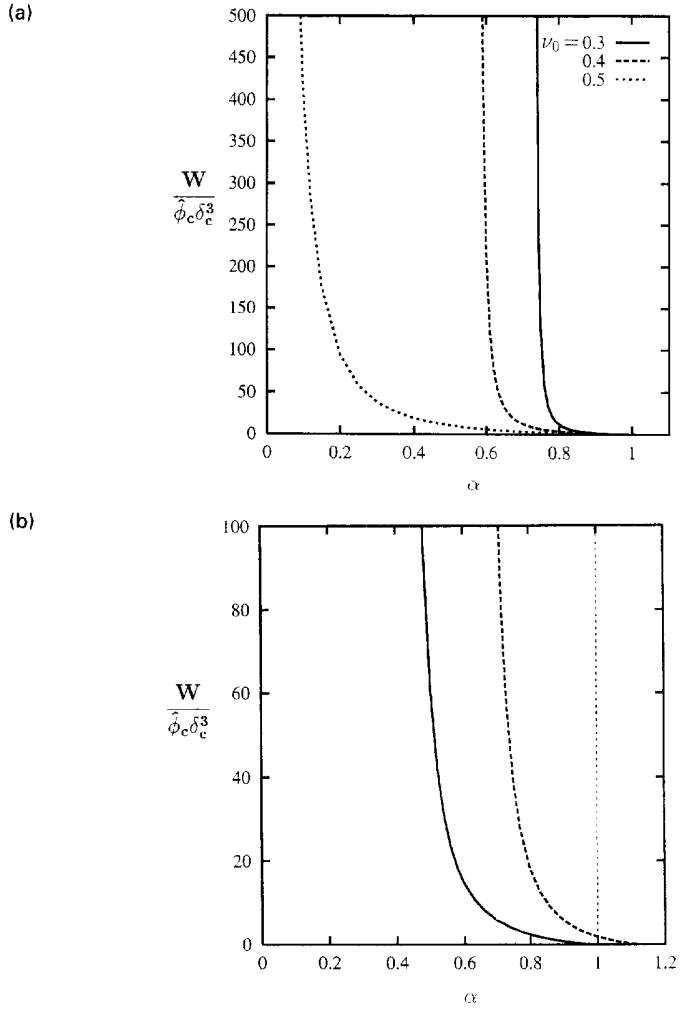

Fig. 6. (a) Nucleation energy W of the critical nucleus, normalized with respect to $\hat{\phi}_c \delta_c^3$, as a function of normalized driving force α with linearly α dependent shear modulus for $\nu_0 = 0.3$, 0.4 and 0.5. (b) Nucleation energy W of the critical nucleus, normalized with respect to $\hat{\phi}_c \delta_c^3$, as a function of normalized driving force α with $\nu_0 = 0.45$; the solid line for $\mu = \mu_0(1-\alpha)$ and the dashed line for $\mu = \mu_0$.

($\alpha = \alpha_i = 1$) is approached. Hence, nonclassical nucleation is energetically favored, particularly close to the instability temperature. The case with the higher initial Poisson's ratio costs less energy for nucleation of the dilatational transformation. Close to $\alpha = \alpha_c$, the dependence of the energy barrier on the normalized driving force is $W \sim (\alpha - \alpha_c)^{-2.0}$, based on data of $\bar{W} = W/(\hat{\phi}_c \delta_c^3) = 7954$ and 3754 at $\alpha = 0.734$ and 0.735 respectively for $\nu_0 = 0.3$; $\bar{W} = 11490$ and 2185 at $\alpha = 0.575$ and 0.58 respectively for $\nu_0 = 0.4$ and $\bar{W} = 43850$ and 10890 at $\alpha = 0.01$ and 0.02 respectively for $\nu_0 = 0.5$. The exponent is equal to the theoretical value, -2, and consistent with the classical theory. Close to the instability temperature ($\alpha = \alpha_i = 1$), the nucleation energy barrier goes as $W \sim (1-\alpha)^{1.50}$, based on data of $\bar{W} = 3.285 \times 10^{-3}$ and 1.159×10^{-3} for $\nu_0 = 0.3$, $\bar{W} = 2.276 \times 10^{-3}$ and 8.039×10^{-4} for $\nu_0 = 0.4$ and $\bar{W} = 1.543 \times 10^{-3}$ and 5.455×10^{-4} for $\nu_0 = 0.5$ at $\alpha = 0.998$ and 0.999 respectively. This exponent is equal to the theoretical value, 1.5, and also consistent with the result predicted by Cahn and Hilliard (1959). A significant difference between the classical nucleation theory and the present model is that the energy barrier of the classical theory remains finite even at the instability temperature.

In Fig. 6(b), the nucleation energy W of the critical nucleus, normalized with respect to $\hat{\phi}_c \delta_c^3$, is plotted as a function of normalized driving force, α, with the initial Poisson's ratio $\nu_0 = 0.45$ for different temperature dependencies in the shear modulus. It can be seen

that, for the case of constant shear modulus, the nucleation energy does not go to zero at $\alpha = 1$, but rather has the value $1.843\hat{\phi}_c\delta_c^3$. This means that nucleation for the case of constant shear modulus is more classical than for the case of the linearly α dependent shear modulus. Close to the coherent equilibrium temperature, both cases depend on the normalized driving force according to $W \sim (\alpha - \alpha_c)^{-2.0}$, based on data of $\bar{W} = 18490$ and 4201 at $\alpha = 0.408$ and 0.414 respectively for linearly α dependent shear modulus and $\bar{W} = 9187$ and 3466 at $\alpha = 0.64$ and 0.645 respectively for constant shear modulus. The exponent is equal to the theoretical value, -2, and consistent with the classical theory.

5. DISCUSSION AND CONCLUSION

The problem of nucleation of a solid-solid displacive phase transformation has been addressed within a finite element framework. A nonlinear, nonlocal (in the sense of gradient energy) material model based on a Landau–Ginzburg type potential is used. A generalization of the one-dimensional Olson–Cohen (1982) model to a spherical geometry has been presented. The spherically symmetric problem represents a genuine three-dimensional state of deformation albeit one of high symmetry. Although the problem depends upon a single spatial variable only, several issues arise which are not encountered in the strictly one-dimensional problem considered by Olson and Cohen (1982). One significant difference between the spherical and one-dimensional models is in the specification of boundary conditions. To generate non-trivial solutions with nucleus structure, the strain can be specified at the nucleus center in the one-dimensional problem (Olson and Cohen, 1982) but not in the spherical problem considered here. Here, the finite element method, together with a perturbed Lagrangian method, is used to obtain the non-trivial solution of interest corresponding to the critical nucleus. An additional difference is the role of shear accommodation in the parent phase. A non-homogeneous dilatational deformation field is accompanied by deviatoric strains. The results of the present paper illustrate that shear (deviatoric) accommodation energy inhibits the nucleation of a dilatational phase transformation, since the required driving force increases as the ratio of the shear modulus to the bulk modulus increases.

The numerical results for various features of interest are consistent with the theoretical analyses at the coherent equilibrium and instability temperatures which are also consistent with the well-known nonlocal Cahn–Hilliard theory for nucleation in a two-component fluid (Cahn and Hilliard, 1959). Thus the results shown illustrate the key features associated with not only classical nucleation but also the nonclassical nucleation.

In the numerical calculations, different values of initial Poisson's ratio were chosen to demonstrate the influence of the deviatoric deformation on the nucleation behavior of the dilatational transformation. The material with a lower value of initial Poisson's ratio requires a higher driving force for nonclassical nucleation, since the ratio of the shear modulus to the bulk modulus increases with decreasing Poisson's ratio. Different temperature dependencies for the shear modulus are also considered. The case of constant shear modulus behaves in a more classical fashion than does the case of temperature dependent shear modulus.

Work in progress consists of a generalization of the present procedure to the treatment of martensitic nucleation.

Acknowledgements—The authors are grateful for the support of the National Science Foundation through grant No. MSS-9313233 to Northwestern University and to P. Hong for helpful discussions. Helpful comments from the reviewers are also gratefully acknowledged.

REFERENCES

Abeyaratne, R. and Knowles. J. K. (1990). On the driving traction acting on a surface of strain discontinuity in a continuum. *J. Mech. Phys. Solids* **38,** 345–360.

Alexiades, V. and Aifantis, E. C. (1986). On the thermodynamic theory of fluid interfaces: infinite intervals, equilibrium solutions and minimizers. *J. Coll. Interf. Sci.* **111,** 119–132.

Ball, J. M. and James, R. D. (1987). Fine phase mixtures as minimizers of energy. *Arch. Rational Mech. Anal.* **100,** 13–52.

Barsch, G. R. and Krumhansl, J. A. (1984). Twin boundaries in ferroelastic media without interface dislocations. *Phys. Rev. Lett.* **53,** 1069–1072.

Barsch, G. R. and Krumhansl, J. A. (1988). Nonlinear and nonlocal continuum model of transformation precursors in martensites. *Met. Trans.* **19A,** 761–775.

Budiansky, B. and Truskinovsky, L. (1993). On the mechanics of stress-induced phase transformation in zirconia. *J. Mech. Phys. Solids* **41,** 1445–1459.

Cahn, J. W. and Hilliard, J. E. (1959). Free energy of a nonuniform system. III. Nucleation in a two-component incompressible fluid. *J. Chem. Phys.* **31,** 688–699.

Christian, J. W. (1975). *The Theory of Transformations in Metals and Alloys*, 2nd ed., Pergamon, Oxford, U.K.

Cohen, M., Olson, G. B. and Clapp, P. C. (1979). On the classification of displacive phase transformations. In *Proc. ICOMAT-79*, pp. 1–11, MIT.

Falk, F. (1983). Ginzburg–Landau theory of static domain walls in shape-memory alloys. *Z. Phys. B-Condensed Matter* **51,** 177–185.

Fisher, J. C., Hollomon, J. H. and Turnbull, D. (1949). Kinetics of the austenite martensite transformation. *Trans. AIME* **185,** 691–700.

Fried, E. and Gurtin, M. E. (1994). Dynamic solid-solid transitions with phase characterized by an order parameter. *Physica D* **72,** 309–323.

Haezebrouck, D. M. (1987). Nucleation and growth of a single martensitic particle. Sc.D. thesis, Massachusetts Institute of Technology.

Hong, P. (1994). Nonclassical displacive transformation mechanics using Fe-Pd as a model system. Ph.D. thesis, Northwestern University.

Kaufman, L. and Cohen, M. (1958). Thermodynamics and kinetics of martensitic transformations. In *Progress in Metal Physics*, Vol. 7 (edited by B. Chalmers and R. King) pp. 165–246, Pergamon Press, New York.

Lusk, M. (1994). On martensitic phase nucleation with surface effects. *J. Mech. Phys. Solids* **42,** 241–282.

Mindlin, R. D. (1965). Second gradient of strain and surface-tension in linear elasticity. *Int. J. Solids Structures* **1,** 417–438.

Olson, G. B. and Cohen, M. (1982). Classical and nonclassical mechanisms of martensitic transformations. *J. Phys.* **43,** C4-75.

Olson, G. B. and Roitburd, A. L. (1992). Martensite nucleation. In *Martensite* (edited by G. B. Olson and W. S. Owen), ASM International.

Porter, D. A. and Easterling K. E. (1992). *Phase Transformations in Metals and Alloys*, 2nd ed., Chapman and Hall, London.

Roitburd, A. L. (1978). Martensitic transformation as a typical phase transformation in solids. In *Solid State Physics*, Vol. 33 (edited by H. Ehrenreich, F. Seitz and D. Turnbull), pp. 317–390, New York, NY Academic.